8.A *Nuclear Physics* **14** (1959/60) 522—539; © *North-Holland Publishing Co., Amsterdam*

MECHANISM OF INTERACTION OF FAST PROTONS WITH NUCLEONS AND NUCLEI

V. S. BARASHENKOV, V. A. BELIAKOV, V. V. GLAGOLEV, N. DALKHAZHAV, YAO TSYNG SE, L. F. KIRILLOVA, R. M. LEBEDEV, V. M. MALTSEV, P. K. MARKOV, M. G. SHAFRANOVA, K. D. TOLSTOV, E. N. TSYGANOV and WANG SHOU FENG

Joint Institute of Nuclear Research, Dubna, USSR

Received 20 March 1959

Abstract: Angular and energy characteristics of interaction between 9 GeV protons and emulsion nuclei, as well as the production of strange particles have been investigated. The obtained experimental results reveal a better agreement with the cascade mechanism of nucleon-nucleus interaction than with the nucleon-tube model.

The average energy loss in a single nucleon-nucleon collision is estimated to be (40 ± 10) %. The size of a nucleon core is discussed. Through the optical analysis of nucleon-nucleon interactions the value $r_c \approx 0.6\times10^{-13}$ cm is obtained for the size of the nucleon core, while the fraction of peripheral collisions constitutes $\approx$ 20 %. Angular and energy distributions of slow K^+ and $\pi^\pm$ mesons have also been obtained. The production cross-section for K^+ mesons with energy up to 140 MeV on an average emulsion nucleus is $\sigma = 5\pm2$ mb.

1. Introduction

The interaction of fast nucleons with nuclei has been studied by many investigators both in the beam of accelerated particles (with energy $E \leqq 9$ GeV) and in cosmic rays [1]). The present work attempts an analysis of experimental results on the interaction of the 9 GeV protons with emulsion nuclei. The preliminary data were reported at the Geneva conference [2]).

In analysing nucleon-nucleus interactions two important factors should be kept in mind:

Firstly, the initial stage of proton-nucleus interaction may be represented either as a proton-nucleon collision or as an interaction of the proton with several nucleons of the nucleus simultaneously — the so called "tube" or "tunnel" which the incident proton cuts out in the nucleus. In the latter case the nucleon of the "tunnel" loses its individuality and the features of the initial stage must depend on atomic number. The conditions leading to "tube" interaction were formulated by E. L. Feinberg [3]). I. A Ivanovskaya *et al.*[4]), in analysing the results obtained in cosmic ray studies, came to the conclusion that the experimental data are consistent with the "tube "model.

Secondly, one should take into account the subsequent intranuclear interactions of particles produced in the first encounter. The probability of such interactions increases with atomic number.

Owing to these factors the interaction of a nucleon with light nuclei considerably differs from the interaction with heavy nuclei. The mechanisms of excitation and subsequent disintegration in light and heavy nuclei also have a number of distinctive features.

Therefore, in our analysis we divided all the observed nuclear interactions produced by incident protons in stripped emulsions into two groups:

1. interactions with light nuclei (C, N, O),
2. interactions with heavy nuclei (Ag, Br).

These groups differ in the number of nucleons by a factor of 7 and in the size of nuclei almost by a factor of 2.

2. Experimental Results

The greater part of the results analysed in this work was obtained with stack "A" consisting of 100 stripped emulsions NIKFI-R, 450 microns thick and 10×10 cm wide, the remaining part — with stack "B" similar to stack "A". These stacks were exposed to the internal beam of 9 GeV protons from the synchrophasotron of the Joint Institute of Nuclear Research.

The following notations are used:

s: shower particles with ionization $I \leqq 1.4\, I_0$, where I_0 is the ionization loss of 9 GeV protons;

g: particles with $I > 1.4\, I_0$ and a range $R > 3.73$ mm (grey tracks);

b: particles with $R \leqq 3.73$ mm (black tracks).

The s-particles consist mainly of pions produced in collision of particles within the nucleus, and of a small fraction of protons (≈ 0.5 per star); g and b particles are for the most part nuclear disintegration products.

The following criteria were used for singling out interactions with light nuclei:

a) the number of grey and black tracks in the star $n_g + n_b \leqq 7$;

b) the star does not contain any track with $R \leqq 10\mu$ i.e., there is no recoil nucleus;

c) there are no electrons in the residual nucleus disintegration;

d) among all tracks at least one has a range $10\mu < R \leqq 50\mu$.

(The emission from heavy nuclei of α-particles with $R < 50\mu$ is suppressed by the Coulomb barrier, the hardly probable tunnel effect being neglected.)

The criteria for selecting the interactions with heavy nuclei were the following

a) either $n_g + n_b > 8$; or

b) if $n_g + n_b \leqq 8$, the star should contain a recoil nucleus, i.e., a track with $R \leqq 10\mu$, and should not contain any track with $10\mu < R \leqq 50\mu$.

Thus, 53 stars out of 1260 found in track scanning and 66 stars out of 2060 found in area scanning were attributed to interactions with light nuclei; this constitutes 3.6 % of all stars. The experimental data obtained by other

investigators [5]) and the optical model analysis of the cross-section show that the interactions with light nuclei should constitute 25—30 % of the total number of interactions. Consequently, the chosen selection criteria are sufficiently rigid.

According to the above criteria, 67 stars out of 100 found in track scanning were ascribed to interactions with heavy nuclei. The obtained characteristics of interactions for light and heavy nuclei and for mixtures of nuclei found in track scanning are given in table 1:

TABLE 1

Characteristics of the interaction between 9 GeV protons and emulsion nuclei

	Light nuclei (C, N, O)	Heavy nuclei (Ag, Br)	Stars with $n_g+n_b \geqq 28$	Mixture of nuclei
$\bar{n}_s$	3.0± 0.2	3.5± 0.3	4.0±0.4	3.2± 0.2
$\bar{n}_g$	1.4± 0.1	4.1± 0.5	32	3.1± 0.4
$\bar{n}_b$	3.3± 0.1	6.1± 0.6		4.7± 0.5
$\theta^0_{s,\frac{1}{2}}$	22.5± 1	27.5± 1.5	53	25.0± 1.5
$\theta^0_{g,\frac{1}{2}}$	56.5± 3	65 ± 3	63	65 ± 3
$\theta^0_{b,\frac{1}{2}}$	—	84 ± 3	—	84.5± 3
$E_{s,\pi}$ (GeV)	—	—	—	1.0± 0.2
$E_{s,p}$ (GeV)	—	—	—	3.0± 0.5
$E_{g,\pi}$ (MeV)	—	—	—	40 ± 3
$E_{g,p}$ (MeV)	132 ±20	118 ±12	—	120 ±12
E_b (MeV)	≈6	12 ± 2	—	11 ± 1.0
$\bar{P}_{g\perp,p}$ (MeV/c)	344 ±20	354 ±20	—	350 ±20
$\bar{P}_{s\perp,\pi}$ (MeV/c)				370 ±70

1. the average numbers $\bar{n}_s$, $\bar{n}_g$, $\bar{n}_b$ of charged particles per star;

2. the angles $\theta_{s,\frac{1}{2}}$, $\theta_{g,\frac{1}{2}}$, $\theta_{b,\frac{1}{2}}$ which contain half of all particles, determined from the angular distributions plotted in figs. 1, 2, 3;

3. the mean kinetic energy for the different kinds of particles;

4. the average transverse momenta for pions and protons. The kinetic energies E_g and E_b for g and b particles were determined from the experimental energy distributions. Fig. 4 shows the energy distribution of g-particles for light and heavy nuclei. The energies of all stopping particles were determined from their range on the assumption that they are all either pions or protons †. The energy distribution of the escaped g particles as well as that of s particles was determined by ionization and multiple scattering measurements (see Appendix).

The average transverse momenta $\bar{p}_{s\perp,\pi}$ and $\bar{p}_{g\perp,p}$ for pions and protons

† The range-energy curves for the Ilford G-5 emulsions were used. The validity of these curves for the NIKFI-R emulsion is proved by the fact that the ranges of μ mesons from the π—μ decays agree well for both types of emulsions.

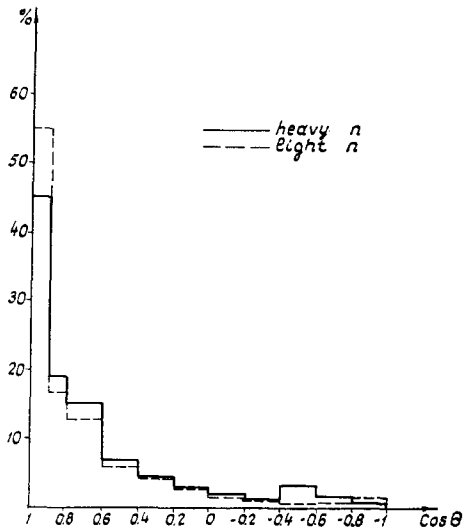

Fig. 1. Angular distribution of 3 particles. The solid line is for heavy nuclei, the dotted line for light nuclei.

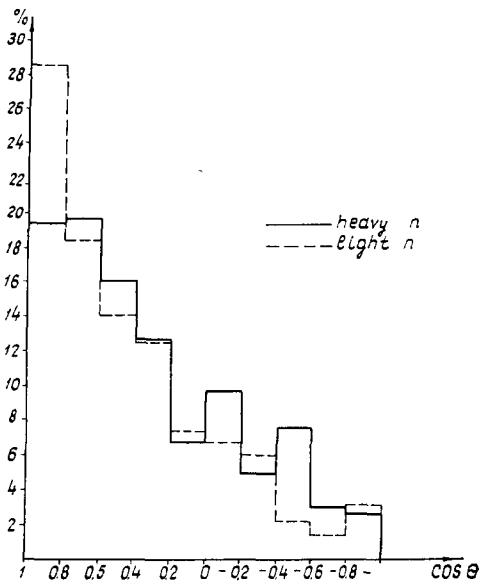

Fig. 2. Angular distribution of g particles. The solid line is for heavy nuclei, the dotted line for light nuclei.

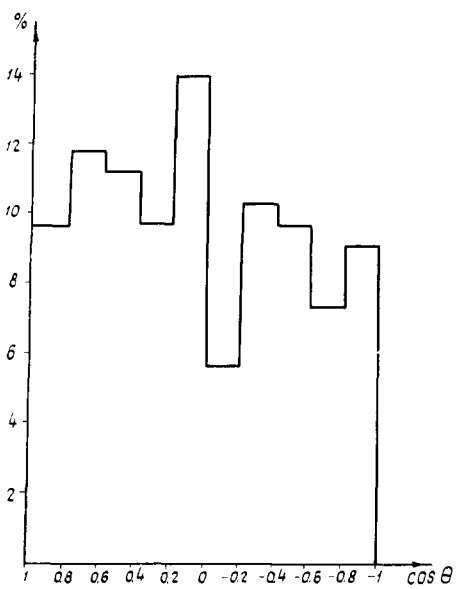

Fig. 3. Angular distribution of g particles on heavy nuclei.

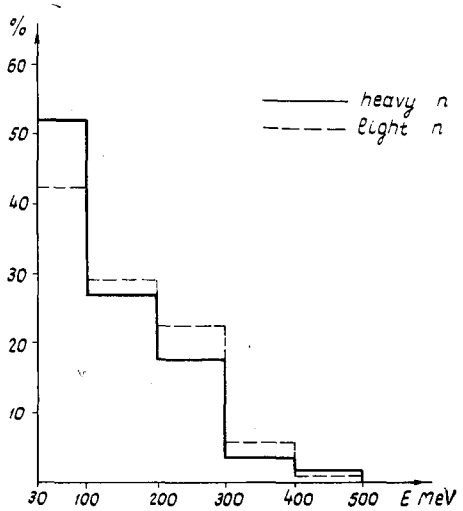

Fig. 4. Energy spectrum of g particles. The solid line is for heavy nuclei, the dotted line for light nuclei.

were obtained from the experimental values of their energies and angles. The values of average transverse momenta for nucleon-nucleon collisions calculated on statistical theory are 0.6 GeV/c and 0.45 GeV/c for nucleons and pions respectively.

The above-enumerated features of interactions with light and heavy nuclei and mixtures of nuclei allow us to calculate the overall energies ε_s, ε_b, ε_g carried away by s, b and g particles per star. The energy ε_g is given by

$$\varepsilon_g = (1+\eta)n_g(E_g+E_N)$$

where η is the ratio of the number of neutrons to protons, and E_N the average binding energy of a nucleon in the nucleus. The energy ε_b was calculated on the assumption either that all B particles are protons, or that the fraction of α particles consitutes 0.2—0.3 of the number of b particles [8]): in both cases ε_b happens to be practically the same.

The values for the energies ε_s, ε_g and ε_b, as well as for the energy $W = \varepsilon_g+\varepsilon_b$ transferred to the nucleus, are given in table 2 for the light, heavy and average nuclei of the emulsion.

TABLE 2

Values of energy $E_s E_g$ and E_b carried away by s, g and b particles and of energy $W = E_g+E_b$ transferred to the nucleus

	Mixture of nuclei	Heavy nuclei	Light nuclei
E_s (GeV)	7.5± 1.0	—	—
E_b (MeV)	180 ± 18	245± 25	≈90
E_g (MeV)	870 ± 90	1165±120	390±50
W (MeV)	1050 ±100	1410±140	480±60

It should be noted that for the light nuclei our value $W_l = 480\pm60$ MeV is in good agreement with the figure 440 ± 160 MeV obtained by N. L. Grigorov [9]) for cosmic ray radiation. It was also indicated by N. L. Grigorov that with variation of the incident particle (proton) energy within the 3—40 GeV range, W_l changes but little.

3. Mechanism of Interaction with Nucleus

It was pointed out in the introduction that a fast proton may interact either with a "tube" or with individual nucleons in the nucleus. In order to determine which of the two possible mechanisms actually takes place, accurate Monte Carlo calculations of nuclear cascades should be compared with the experimental data. Since such calculations are not yet completed we shall confine ourselves only to some qualitative considerations.

The assumption that the primary nucleon interacts with a "tube" leads to

values of $\theta_{s,\frac{1}{2}}$ angles $\approx 30°$ and $\approx 40°$ for light and heavy nuclei respectively †. These values considerably exceed the experimental ones. The probability of secondary interactions of particles produced in the nucleon-tunnel collision might only increase the calculated values of the angles.

Furthermore, if the initial stage of the nucleon-nucleus collision is a nucleon-tube interaction, the centre-of-mass velocity in the case of interaction with Ag and Br tubes will be much lower than for light nuclei, since on the average the tube is almost twice longer, and consequently the number of s particles must be considerably greater. In the experiments, however, the numbers of s particles produced on heavy and light nuclei are respectively equal to 3.5 ± 0.3 and 3.0 ± 0.2. Such a small difference can be explained by the cascade mechanism of interaction. Indeed, in the case of cascade collisions the energy of s particles decreases rapidly as the cascade proceeds, and this leads to a diminishing multiplicity of particles produced in these collisions.

Besides, the realization of the nucleon-tube mechanism would imply a considerable contamination of g particles by pions produced in the collision of a nucleon with the nuclear tube. The experimental data show, however, that g particles are almost exclusively nucleons, which can again be explained on the assumption of the cascade mechanism of the nucleon-nucleus interaction, according to which the majority of g particles are recoil nucleons. This agrees with the experiments on meson-nucleon collisions at $E > 0.5\,\mathrm{GeV}$ [10]), in which recoil nucleons of an energy corresponding to g particles were observed with a probability near unity.

The tube interaction model is of still less avail in explaining the events of nuclear disintegration with emission of more than 28 g and b particles ($\bar{n}_g+b=32$) which are observed in > 2 % cases and listed in table 1. In these disintegrations a complete decay of a nucleus into protons and neutrons with a small fraction of α-particles takes place, and the $\bar{n}_s$, $\theta_{g,\frac{1}{2}}$ and W values are nearly the same as the corresponding values for all cases of interaction with heavy nuclei.

The fact that the values of the transverse momentum $P_{g\perp}$ coincide for g particles produced on light and heavy nuclei, and also agree with the transverse

† The average number of nucleons in a tube,

$$n = \frac{\text{volume of tube}}{\text{specific volume per nucleon}} \approx \sqrt[3]{A},$$

with due consideration for the emulsion composition, is 2.4 and 4.6 for light and heavy nuclei. In calculating the $\theta_{s,\frac{1}{2}}$ angles a distribution of the produced particles isotropic in the centre of mass system was assumed and the laws of conservation of energy and momentum, baryon number and strangeness were taken into consideration. Account was also taken of the resonance interaction between the generated mesons and nucleons in a state with total and isobaric spins equal to $\frac{3}{2}$ at 200 MeV. Similar, but somewhat lower, values of the $\theta_{s,\frac{1}{2}}$ angles for light and heavy nuclei were also obtained by V. M. Maksimenko; we wish to thank V. M. Maksimenko for making the results of his calculations available to us prior to publication.

momenta of π-mesons (see table 1), also points to the cascade mechanism of interaction.

All other experimental results can also be explained on the assumption of the nuclear cascade.

4. Energy Losses in Nucleon Collisions

For the purpose of determining the average energy of s particles 83 particles with dip angle $< 3°$ were selected. The momenta of those particles were esti-

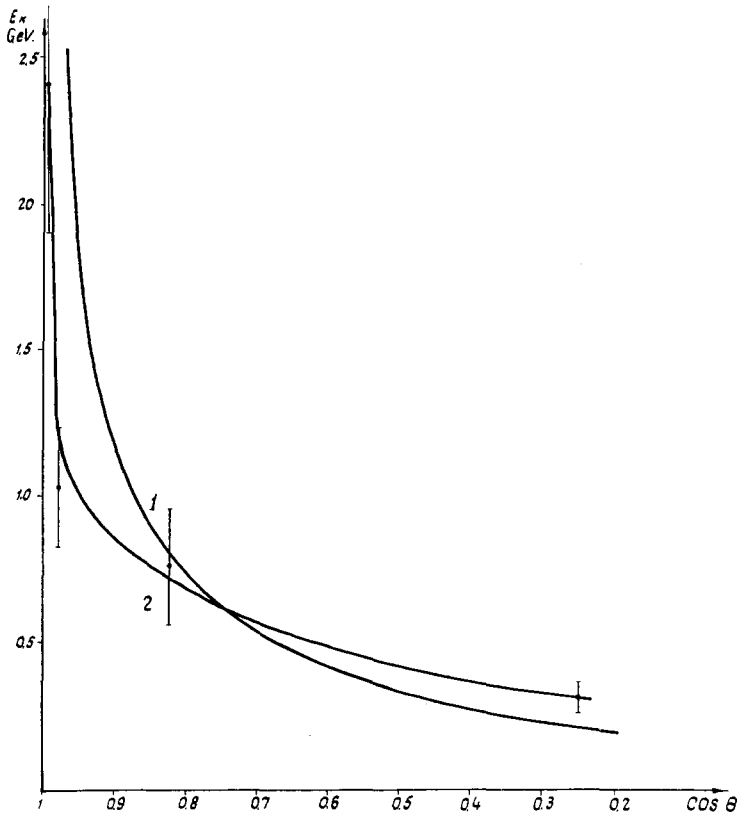

Fig. 5. Curve 2 represents the dependence of pion energy on the emission angle (mixture of nuclei). Curve 1 is a theoretical curve calculated from statistical theory for N—N collisions.

mated by multiple scattering measurements, and their masses were obtained from ionization losses (for more detail see Appendix). In the angular interval of 0—15° the mean energy of the protons was found to be 3 ± 0.5 GeV, while the ratio of the number of pions to the number of protons was ≈ 1, which corresponds to ≈ 0.5 proton per star. Then, the curve of the pion energy dependence

on the angle was obtained as plotted in fig. 5. Using this dependence and the angular distribution of s particles for the mixture of nuclei, and also taking into account the found fraction of protons, we obtained the mean total energy of mesons which, in the 0—30° angular interval, equals $\bar{E}_\pi = 1.3 \pm 0.25$ GeV (measurements were performed with chamber "B", see Appendix). The total energy averaged over all angles is $\bar{E}_\pi = 1.0 \pm 0.2$ GeV. Thus, the energy losses for meson production constitute 4.0 ± 0.8 GeV.

Together with the energy of nuclear disintegration the losses will be equal to 5.1 ± 0.8 GeV, i.e., 60 ± 10 %.

The number of collisions which the incident proton undergoes on the average in a light nucleus can be estimated from the measured values $\bar{n}_s = 3$ and $\bar{n}'_g = 2.8$ (including neutrons). It can be assumed that in the first collision the proton yields one g particle (0.5 proton and 0.5 neutron) and together with neutral mesons the total number of fast particles is

$$\bar{n}'_s = \tfrac{3}{2}(\bar{n}_{s,p} - 0.5) + 1 = 4.3,$$

where $\bar{n}_{s,p}$, the average number of s particles in proton-nucleon collisions, is [13]) equal to 2.7 (the coefficient $\frac{3}{2}$ takes into account the fraction of neutral pions). The number of secondary collisions will be

$$\frac{\bar{n}'_g - 1}{\bar{n}'_s} = 0.4.$$

Consequently, the primary proton on the average undergoes 1.4 collisions in a light nucleus. The number of collisions with Ag and Br nuclei, in accordance with the nucleus size, can be taken to be two times greater. Hence, on the average, the proton undergoes $\gtrsim 2$ collisions in the emulsion nucleus.

If the nucleon energy after one nucleon-nucleon collision is $E_1 = \xi E$, where E is the initial energy of the nucleon, then, after n collisions, the nucleon energy is $E_n = \xi^n E$. With $n = 2$, we obtain that the average energy loss in one nucleon-nucleon collision constitutes 35 ± 10 %.

The energy losses in nucleon-nucleon collisions can also be estimated in the following way. We have derived that the mean total energy of pions produced in collisions with nuclei is 1.0 ± 0.2 GeV. The experimental value $\bar{n}_s$ for p—p collisions was obtained in ref. [11, 12]). Considering that the mean pion energy in nucleon-nucleon collisions cannot be lower than in nucleon-nucleus collisions and that s particles contain ≈ 0.5 proton, we deduce that the energy loss in a nucleon-nucleon collision must be $\geqq 40 \pm 10$ %. Within the limits of experimental errors this value is not in contradiction with the theoretical one of 50 % obtained in statistical theory [12]). Peripheral collisions may slightly reduce this value.

It should be noted that in cosmic ray studies [9]) the average energy losses of a nucleon in collisions with air nuclei were found to be 30 ± 3 % in the 3—40 GeV

energy range. If the number of collisions in an average nucleus of the air is taken to be equal to 1.5, the energy losses for a single nucleon-nucleon collision must constitute 20 % of the primary particle energy.

The results obtained above, as well as the previously published data on nucleon interactions [12]) make it possible to offer some considerations pertaining to the size of the nucleon core.

The paper just mentioned [12]) reported some results on the nucleon-nucleon interactions at 9 GeV. It was shown that on the whole there is agreement with the statistical theory of multiple production [7]). However, there is a discrepancy in the region of small angles pointing to anisotropy in the centre of mass system. Similar experimental results were obtained by N. P. Bogachev *et al.* [11]). Further work [13]) established that only for stars with a small number of particles does anisotropy of angular distribution occur in the centre of mass system. The angular distribution of prongs in stars with a great multiplicity of particles may be considered isotropic within experimental errors.

In terms of a nucleon model consisting of a central core and peripheral meson cloud collisions with great multiplicity can be considered as core collisions. The statistical theory of multiple production is applicable for describing such collisions. As to the collisions with small multiplicity, they can be regarded as collisions of the core of one nucleon with the periphery of another, or as peripheral collisions of nucleons. Since the experimental number of s particles, their energy, angular distribution (with the exception of small angles) and the energy losses agree in the main with the statistical theory calculations, we are led to conclude that nucleon-nucleon collisions at $E \leqq 10$ GeV are for the most part collisions of their cores.

The optical analysis of proton-nucleon collisions in the 1—10 GeV energy range has shown that they occur with the greatest probability for an impact parameter

$$b = \lambda\!\!\!^{-}\sqrt{l(l+1)}$$

approximately equal to 0.6×10^{-13} cm. (There , $\lambda\!\!\!^{-}$ is $(2\pi)^{-1}$ times the wavelength in the centre of mass system, and l the corresponding angular momentum.) This can be seen from fig. 6, which represents the relative contribution to the cross-section of inelastic proton-proton collisions:

$$\Delta = \frac{\sigma_{\text{in}}(b)}{\sigma_{\text{in}}} = \frac{(2l+1)(1-e^{-4\eta(l)})}{\sum_{l=0}^{\infty}(2l+1)(1-e^{-4\eta(l)})},$$

due to interaction in the region b, $b+\lambda\!\!\!^{-}$, at energies $E = 1.5$, 4.4 and 10 GeV †, i.e. $\lambda\!\!\!^{-} = 0.24$, 0.14 and 0.091×10^{-13} cm.

† The values of absorption and refraction coefficients $K(r)$ and $U(r)$ are taken from ref. [6]). At 10 GeV, σ_{in} is assumed to be equal to 30×10^{-27} cm^2 in accordance with the results of ref.[14]).

If nucleon-nucleon collisions at 9 GeV are mainly collisions of the cores, we thus infer that the radius of a nucleon core r_c is $>\frac{1}{2}b$, i.e., $r_c > 0.3 \times 10^{-13}$ cm, which agrees with the analysis of the electromagnetic size of the core [15]).

If one accepts that core collisions are most probable for the impact parameter $b \approx r_c$, then r_c is $\approx 0.6 \times 10^{-13}$ cm. (The latter value gives the limit between large and small values of the absorption coefficient $K = K(r)$ [16]).) In this case the contribution of peripheral collisions constitutes ≈ 20 %. It should be noted that the anisotropy of angular distributions revealed by the experiments may

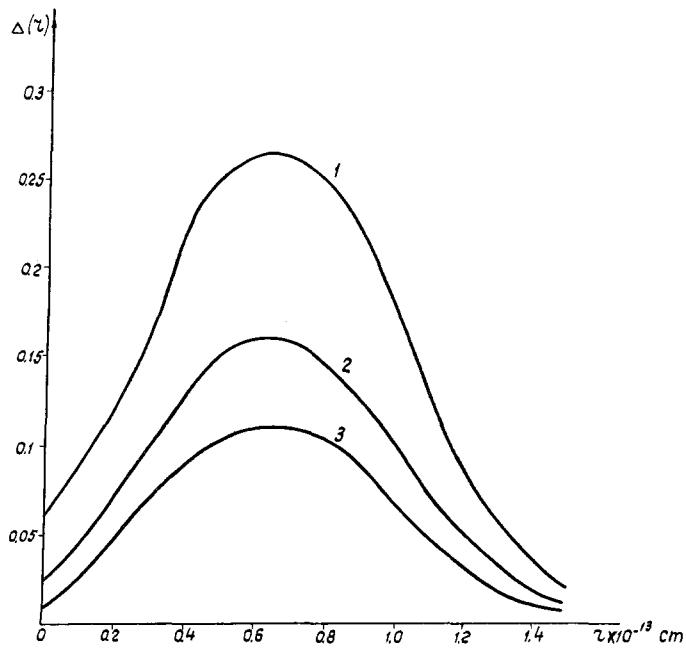

Fig. 6. Relative contribution to the cross-section of inelastic N—N collisions which is due to the interaction in the region $(b, b+\lambda\!\!\!^{-})$. The curves 2, 1, 3 describe the collisions at 1.5, 4.4, 10 GeV respectively (in the laboratory system).

in some part be due to the conservation of angular momentum. Both effects are being calculated at present.

The value of 80 % obtained in ref. [17]) for peripheral collisions was based on the unsound assumption that

$$\sigma_{\text{periph}} : \sigma_{\text{integral}} = \pi r_c^2 : \pi r_N^2, \qquad r_N \approx 10^{-13} \text{ cm}$$

(cf. the graph $K = K(r)$ in ref. [16])), as well as on an inaccurate choice of the values of constants.

5. Production of Slow Strange Particles and Pions

In following up all prongs of the 100 stars found in track scanning not a single strange particle was registered. The systematic search for strange particles was carried out by area scanning. All the marked part (a circle 8.5 cm in diameter) of the 15 emulsion strips was twice scanned under the 200× magnification. The efficiency of single scanning was equal to 88 % for primary stars and 80 % for secondary stars. Altogether 2322 primary and 2361 secondary

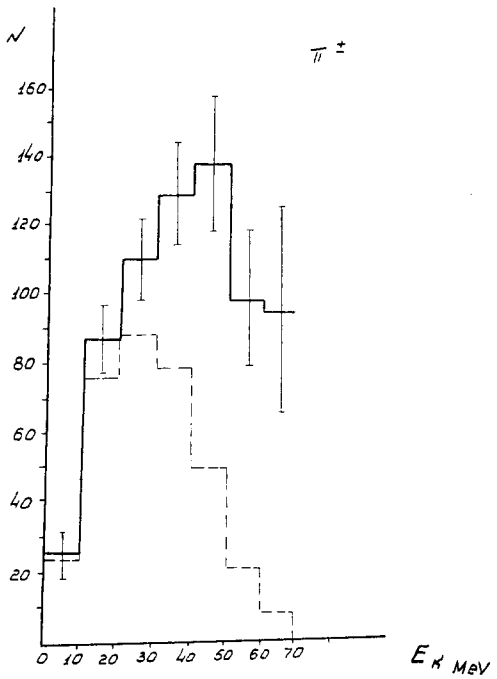

Fig. 7. Angular distribution of $\pi^{\pm}$ mesons. Solid curve includes geometrical corrections.

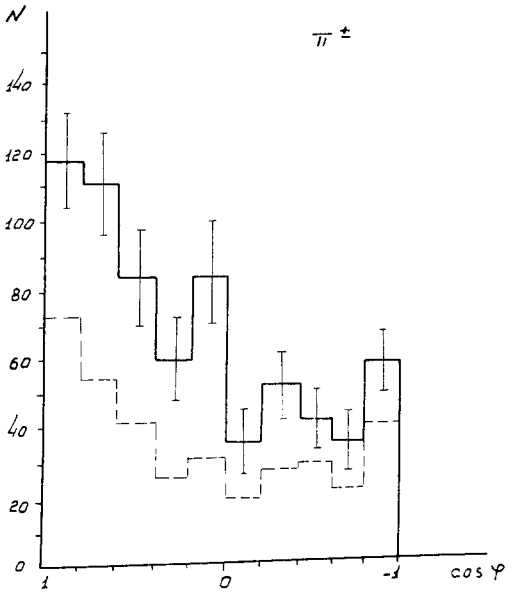

Fig. 8. Energy distribution of $\pi^{\pm}$ mesons. Solid curve includes geometrical corrections.

stars were found. In scanning 18 emulsions 387 stars and 386 $\pi^+ - \mu - e$ decays were detected. In following up these meson tracks it was discovered that 203 π^- and 146π^+ mesons were generated in the primary stars of the marked area of the chamber. Angular and energy distributions of these mesons proved to be similar. Their spectra were calculated with the corrections for the escapes due to the finite size of the chamber. These corrections were introduced by the method described in ref. [18]). Figs. 7 and 8 represent angular distributions of π^+ and π^- mesons and their energy spectrum with and without the geometrical corrections (solid and dotted lines respectively).

For the purpose of singling out strange particles all the two-prong events

were analysed. Identification was effected through the residual range and ionization by the method of blob and gap count. 32 strange particles were detected: 22 K^+ mesons, 1 K^-, 4$\Sigma^\pm$ hyperons and 5 Λ° particles. The values of their emission angles with respect to the beam and their kinetic energy are given in table 3. Only 18 parent stars were found for all strange particles (from among

TABLE 3

Summarized data on strange particles †

	Particle type	Parent star type $(n_g+n_b)+n_s$	Angle θ with respect to the proton beam	E_{kin} (MeV)	Q (MeV)	Remarks
1	K^+	8+4	150	84.9		
2	K^+	25+6	80	107		
3	K^+	15+5	0	10.7		
4	K^+	24+6	50	66		
5	K^+	12+6	43	54		
6	K^+	8+8	1	48		
7	K^+	16+2	95	22.6		
8	K^+	8+1	91	71		
9	K^+	5+2	47	44		
10	K^+	23+8	14	96		The parent star is outside the marked area
11	K^+	15+7	95	90		
12	K^+	14+3	102	38		
13	$\Sigma^\pm$	21+4				
14	$\Sigma^\pm$	10+1	6			
15	$\Sigma^\pm$	18+5	79	168		
16	Λ^0	17+6	90	8	36.6	Found in area scanning and in following pion track; the range is 13.5 mm
17	Λ^0	23+6	160	27	37.3	The range is 10.5 mm
18	Λ^0	13+1	135	67	37.4	The range is 13 mm

† The table lists events which have parent stars.

them parent stars for 3 Λ° particles). For these stars $\bar{n}_g+\bar{n}_b = 15.6\pm4$, $n_s = 4.2\pm1.2$. These values exceed the average characteristics of stars found in track scanning. One event of simultaneous production of 2 strange particles was registered. Out of 22 K^+ mesons 12 were generated in primary stars and their mean energy equals 61 MeV. We shall now determine the cross-section of the K^+ production for this part of the spectrum. The efficienty of detecting the K^+ type events was estimated in the following way. All the two-prong events containing s and b or g particles (including K meson decays) were selected, the total number amounting to 57. Out of this number 37 relativistic particles are emitted in the interval of dip angles $0^\circ \leqq \alpha \leqq 36^\circ$ (0.59 of the total solid angle). If the angular distribution of these particles is isotropic 64.5 events ought to be observed, whence the relative efficiency over different dip angles is 0.88. A similar analysis of black prongs led to a relative efficiency of 0.90. It remains then to determine the detection efficiency for the events with the

black and relativistic prongs contained in the angular interval $0^0 \leqq \alpha \leqq 36°$. This efficiency was obtained by independent double scanning of one and the same emulsion area and was found to be 0.85.

The average density of the proton flux was equal to $(3.1 \pm 0.3) \times 10^3$ cm^2. The number of nuclei in one cm^3 of the emulsion is 7.83×10^{22}. Thus, the production cross-section for K^+ mesons with energy up to 140 MeV, on the average emulsion nucleus, corresponds to (5 ± 2)mb (with geometrical corrections). The angular distribution of the 12 K^+ mesons (also with geometrical correc-

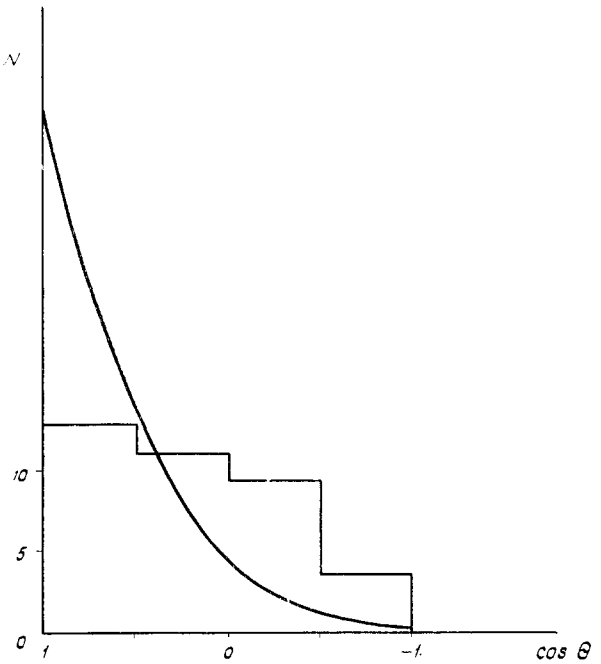

Fig. 9. Angular distribution of K^+ mesons produced in N—N collisions. The curve is calculated from the statistical theory.

tions) is given in fig. 9. The statistical theory curve for the angular distribution of K mesons produced in p—p collisions is plotted in the same figure. Comparison of the experimental and theoretical curves reveals a large discrepancy, which is difficult to explain only by K meson scattering in nuclei.

Indeed, in the energy interval up to 300 MeV the mean free path of K mesons in nuclear matter is 11×10^{-13} cm [19]). If we assume that the majority of K mesons was produced on heavy emulsion nuclei, and take their range to be of the order of the nuclear radius $1.2A^{\frac{1}{3}} \times 10^{-13}$ cm, we obtain that the number of interactions within the nucleus will be $< 1.2\sqrt[3]{94/11} \approx 0.5$ i.e., much less than for π mesons.

The combination of such facts as the high value of the production cross-

section, wide angular distribution and large size of parent stars support the inference that the greater part of strange particles is produced in the intranuclear cascade process, which is quite probable in view of the value ≈ 1 GeV for the mean energy of mesons. A similar conclusion was reached by C. Besson *et al.*[20]) who investigated the production of strange particles by π^- mesons at 4.3 GeV.

In conclusion the authors wish to thank G. Beznogikh, Z. Kuznetsova, N. Metkina, M. Prisnolova and V. Vaksina who were very helpful in scanning and also to acknowledge the aid in analysis by L. Popova. They would also like to express their gratitude to the Zeiss company, Jena, German Democratic Republic, which has manufactured a first-rate measuring microscope for nuclear research, to professor K. Rambush who was very helpful in making this microsope available to the Joint Institute and in particular to H. Bayer, H. Schüler and M. Sost who were in charge of the delivery and installation.

Appendix

MOMENTUM DETERMINATION FOR STRANGE PARTICLES BY MULTIPLE SCATTERING MEASUREMENTS

The following microscopes were used: MB1—8 with a modernized stage and a noise background $\approx 0.03\mu$ for a 2000μ cell; KSM-Karl Zeiss Jena with noises $\approx 0.008\mu$ for a 2000μ cell; Koristka with noises $\approx 0.02\mu$ for a 2000μ cell. Measurements were performed on two emulsion chambers: chamber "A" whose pellicles were processed in a free state, and chamber "B" whose emulsion strips were stuck to the plates before processing.

The average distortion level and quasi-scattering were evaluated by direct measurements of proton beam tracks. The value 1.5μ on a 1000μ cell was obtained for chamber "A" and 0.65μ on a 2000μ cell for chamber "B".

A rough estimate of the secondary particles energy made from their interaction with emulsion nuclei allowed us to infer that all the strange particles with θ angles $> 30°$ are comparatively slow. Therefore, chamber "A" despite great distortions proved to be suitable for scattering measurements of particles with θ angles $> 30°$.

For these particles the cell length was chosen in such a way that the ratio of the measurement signal to the distortion signal equalled 3 or more and there was no need to introduce corrections for distortion. The momentum of these particles was calculated from the formula

$$|\bar{D}| = \frac{A t^{\frac{3}{2}}}{p\beta c} \tag{1}$$

where $A = 50.6$ for a scattering constant $K = 29$, and t is the cell length in units of 100μ.

TABLE 4

Results of energy measurements of secondary particles on chamber "B'

No.	Space angles $\theta°$	Identification	$E \pm \Delta E$ (MeV)
1	1.9°	proton	$5.3^{+4.3}_{-1.5}$
2	5.9°	proton	$2.1^{+1.2}_{-0.5}$
3	1.5°	proton	$4.7^{+4.5}_{-1.4}$
4	3°	proton	$5.4^{+4.6}_{-1.7}$
5	1.3°	π-meson	$3.6^{+0.7}_{-0.5}$
6	4.5°	proton	$3.2^{+1.6}_{-0.9}$
7	10.3°	proton	$1.9^{+1.0}_{-0.5}$
8	1.3°	π-meson	$3.5^{+1.0}_{-0.5}$
9	7.6°	proton	$3.1^{+1.4}_{-0.9}$
10	3.1°	proton	$3.1^{+1.4}_{-0.9}$
11	0.6°	proton	$3.2^{+0.8}_{-0.6}$
12	1.4°	proton	8
13	10°	probably proton	$5.7^{+2.9}_{-1.5}$
14	1.5°	π-meson	$5.4^{+2.5}_{-1.3}$
15	5°	proton	$7.6^{+14}_{-3.4}$
16	8.1°	proton	$3.5^{+1.2}_{-0.8}$
17	4.4°	π-meson	$2.9^{+0.7}_{-0.5}$
18	4.3°	π-meson	$1.3^{+0.4}_{-0.2}$
19	14.1°	π-meson	$0.86^{+2.0}_{-0.2}$
20	12.4°	π-meson	$0.63^{+0.17}_{-0.14}$
21	6.4°	probably π-meson	$2.1^{+0.5}_{-0.4}$
22	4.8°	proton	$2.0^{+1.0}_{-0.6}$
23	2.4°	proton	$0.52^{+0.16}_{-0.07}$
24	9.7°	π-meson	$0.22^{+0.06}_{-0.03}$
25	22°	probably π-meson	$1.9^{+0.6}_{-0.4}$
26	13.1°	proton	$1.0^{+0.4}_{-0.2}$
27	14.8°	proton	$1.3^{+0.5}_{-0.3}$
28	11°	π-meson	$0.71^{+0.24}_{-0.11}$
29	30°	probably π-meson	$2.2^{+0.9}_{-0.6}$
30	2.2°	π-meson	$1.3^{+0.3}_{-0.2}$
31	9.7°	π-meson	$2.8^{+1.3}_{-0.7}$
32	9.5°	probably π-meson	$1.8^{+0.6}_{-0.4}$
33	11.8°	π-meson	$0.69^{+0.17}_{-0.09}$
34	29.8°	π-meson	$2.5^{+1.1}_{-0.7}$
35	18.8°	π-meson	$0.15^{+0.03}_{-0.03}$
36	5.9°	proton	$0.51^{+0.18}_{-0.06}$
37	9.7°	probably proton	$1.6^{+0.9}_{-0.4}$

TABLE 4
(continued)

No.	Space angles $\theta°$	Identification	$E^{\pm}\Delta E$ (MeV)
38	16.6°	π-meson	$0.88^{+0.17}_{-0.13}$
39	5.3°	π-meson	$1.3^{+0.3}_{-0.2}$
40	15.3°	π-meson	$0.54^{+0.14}_{-0.09}$
41	2.5°	proton	$2.3^{+1.5}_{-0.7}$
42	11.8°	probably proton	$1.1^{+0.5}_{-0.3}$
43	1.6°	probably proton	$1.4^{+0.5}_{-0.3}$
44	2°	probably π-meson	$1.9^{+0.5}_{-0.3}$
45	4°	probably proton	$1.9^{+0.6}_{-0.4}$
46	0.9°	π-meson	$1.4^{+0.3}_{-0.2}$
47	1.1°	proton	$1.1^{+0.3}_{-0.2}$
48	4.2°	π-meson	$0.4^{+0.07}_{-0.05}$
49	13.3°	π-meson	$0.71^{+0.13}_{-0.09}$
50	5.5°	proton	$2.3^{+0.8}_{-0.5}$

Tracks with flat θ angles $< 30°$ were measured on stack "B". Here the particles were divided into two groups: $p\beta c < 2$ GeV and $p\beta c\ 2 > 2$ GeV. The momenta of particles with $p\beta c < 2$ GeV were calculated from formula (1), quasi-scattering was eliminated through the formula

$$\bar{D}^2_{\text{Coul}} = \bar{D}^2_{\text{meas}} - \bar{D}^2_{\text{quasi}}; \tag{2}$$

$\bar{D}_{\text{quasi}}$ was averaged over all emulsion strips in which the measurements were made.

For particles with $p\beta c > 2$ GeV noises and distortions were eliminated through the formula [21, 22])

$$|\bar{D}|_{\text{Coul+quasi}} = 0.715\sqrt{\bar{D}_i^2 + \bar{D}_i\bar{D}_{i+1} - 2\bar{D}_i\bar{D}_{i+2}} \tag{3}$$

and quasi scattering through formula (2). Quasi-scattering was measured on beam particles all along a secondary track, i.e., along five-or six-beam tracks.

All the measurement results are summarized in table 4.

ERRORS

The total error in momentum measurements was respectively made up of the statistical error of direct measurements ($\Delta = 0.86/\sqrt{n}$ in accordance with ref.[1])) and of the error due to the elimination of quasi-scattering.

In determining the nature of secondary particles a blob count method was additionally used. The results are plotted in fig. 10.

The a—a′ lines mark an area in which protons cannot be separated from pions by their ionization. This area contains 9 particles. We roughly estimated

that half of them are protons because in the neighbouring areas the ratio of protons to pions is of the order of a unity.

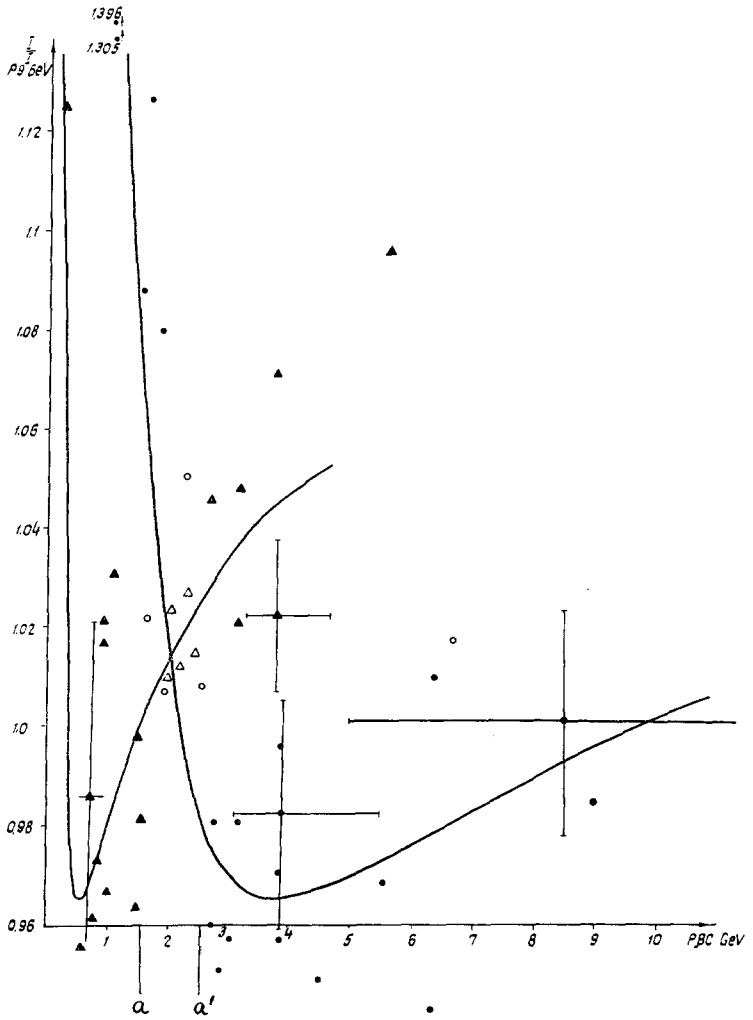

Fig. 10. The momentum versus ionization curves for protons and π^- mesons (on the basis of Barkas' tables) and the experimental data on s particles.
● — proton, ○ — probably proton; ▲ — π meson, △ — probably π meson.

Further, it turned out that among the identifiable particles all protons have angles $\leqq 15°$, therefore the particles with angles $> 15°$ in the a—a′ area were transferred from the proton group to the meson group †.

† It should be noted that the procedure of particle identification in the a—a′ area does not practically affect the obtained value of mean energy, because the energy values in this area are close to the mean energy.

References

1) N. P. Bogachov *et al.*, Atom. Energ. **4** (1958) 281;
W. R. Johnson, Phys. Rev. **99** (1955) 1049
2) V. Beliakov *et al.*, Annual International Conference on High Energy Physics at CERN (1958) p. 309
3) E. L. Feinber, JETP **28** (1955) 241; Usp. Fiz. Nauk **58** (1956) 193
4) I. A. Ivanovskaya and D. S. Chernavsky, Nuclear Physics **4** (1957) 29
5) E. L. Grigoriev and L. P. Solovyova, JETP **31** (1956) 932
6) V. S. Barashenkov and Huan Nian Nin, JETP (in press)
7) V. S. Barashenkov, B. M. Barbashov and E. G. Bubelev, Nuovo Cimento **7**, Suppl. 1 (1958)**117**
8) W. O. Zock, P. V. Murch and R. M. Keague, Proc. Roy. Soc. **231** (1955) 368
9) N. L. Grigorov, Usp. Fiz. Nauk **58** (1956) 599
10) W. D. Walker and J. Crussard, Phys. Rev. **98** (1955) 1416;
J. E. Crew and R. D. Hill, Phys. Rev. **110** (1958) 177;
M. Blan and A. R. Oliver, Phys. Rev. **102** (1956) 489
11) N. P. Bogachev, S. A. Buniatov, Y. P. Merekov and V. M. Sidorov, Dokl. Akad. Nauk SSSR **121** (1958) 617
12) V. S. Barashenkov *et al.*, Nuclear Physics **9** (1958) 74
13) N. P. Bogachev *et al.*, private communication
14) V. S. Barashenkov and Huan Nian Nin, JETP **36** (1959) 1319
15) D. I. Blokhintsev, V. S. Barashenkov and B. M. Barbashov, Usp. Fiz. Nauk (in press)
16) D. I. Blokhintsev, V. S. Barashenkov and V. G. Grishin, Nuovo Cimento **9** (1958) 249; V. G. Grishin, JETP **35** (1958) 50
17) E. G. Bubelev, JETP **33** (1957) 539
18) V. V. Alpers *et al.*, JETP **30** (1956) 1025
19) M. F. Kaplon, Annual International Conference on High Energy Physics at CERN (1958) p. 173
20) C. Besson *et al.*, Nuovo Cimento **6** (1957) 1168
21) B. d'Espagnat, J. Phys. et le Radium **13** (1952) 74; Comptes Rendus **232** (1951) 800
22) A. G. Ekspong, Arkiv för Fysik **9** (1955) 49